Spatial patterns induced in a laser beam by thermal nonlinearities

Sean J. Bentley and Robert W. Boyd

The Institute of Optics, University of Rochester, Rochester, New York 14627

William E. Butler and Adrian C. Melissinos

Department of Physics and Astronomy, University of Rochester, Rochester, New York 14627

Received January 25, 2001

Stable spatial laser patterns were observed in a high-finesse Fabry–Perot cavity containing up to 2 atm of CO_2 and O_2. The gases displayed the same sequence of patterns that obey a scaling law of the form $P^\beta p^2$, where P is the power stored in the cavity, p is the pressure of the gas, and β is a material-dependent parameter. © 2001 Optical Society of America

OCIS codes: 190.0190, 120.2230.

Pattern formation,[1–4] the introduction of transverse spatial structure onto a laser beam by a nonlinear optical process, has received much attention recently. The bulk of this work has been done with high-peak-power, short-pulse lasers, making use of the large intensities to gain access to the electronic nonlinearities that drive the pattern formation. Thermal nonlinearities,[5–8] while often much larger for the same material, can be experimentally difficult to explore because of the need for high-power, cw lasers.

We recently demonstrated[9] a method of gaining access to the thermal nonlinearities of various gases through the use of a stable cw laser locked to a high-finesse Fabry–Perot cavity.[10] Using the same experimental arrangement (Fig. 1), we have observed and studied the formation of stable spatial laser patterns in both CO_2 and O_2. The patterns, examples of which are shown in Fig. 2, are stable in time, reproducible, and can reach very high complexity. Although some of the patterns have a similar structure, the transitions were abrupt and easily identifiable, and examination of the subsequent patterns showed an increasing number of nodes for increasing power or pressure.

The experimental setup (see Fig. 1) consists of a 500-mW cw Nd:YAG nonplanar ring oscillator laser[11] (NPRO) locked to a high-finesse cavity (HFC) containing the gas under investigation. The HFC is made from 1-m radius-of-curvature mirrors with 10-cm spacing. The finesse is 12,000, and the cavity transmission is 12%, providing a power buildup factor inside the cavity of 1300. The cavity mirrors are rigidly mounted to a Zerodur spacer inside a metal cylinder suspended in a vacuum chamber. A Faraday isolator (FI) protects the laser from backreflections. A half-wave plate (HWP) with a polarizing beam splitter (PBS) is used to control the power incident on the cavity. Locking of the laser frequency to the cavity resonance is achieved with a Pound–Drever–Hall feedback system.[12] An electro-optic modulator (EOM) places 40-MHz sidebands on the beam. When the laser frequency is resonant with the cavity, the sidebands are reflected because of the narrow bandwidth of the cavity resonance. The reflected light is redirected by the polarizing beam splitter to the photodiode (D1). The output of D1 is combined with the 40-MHz source via a rf mixer (X). The low-frequency components of the mixer output provide the error signal, which keeps the laser on resonance. The light transmitted by the cavity is split by a nonpolarizing beam splitter (BS), with one half imaged via a lens onto a CCD camera (CCD1) that gives the near-field pattern and the other half falling directly onto a CCD camera (CCD2) that gives the far-field pattern.

We studied several gases, Ar, He, N_2, CO_2, O_2, and N_2O, but observed patterns only in CO_2, O_2, and N_2O. We believe that this is because absorption is much weaker in the first three gases at $\lambda = 1.06\ \mu$m, and thus the patterns could not be observed for the power and pressure levels at which the experiment was

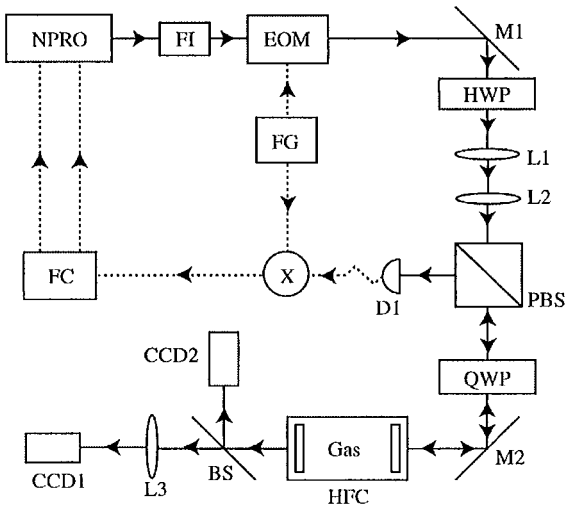

Fig. 1. Schematic of experimental setup. The optical paths are shown as solid lines, and the electrical paths are dotted lines. FC, feedback controls; FG, 40-MHz function generator; M1, M2, mirrors; L1–L3, lenses; QWP, quarter-wave plate. See text for other definitions.

0146-9592/01/141084-03$15.00/0

Fig. 2. Examples of three of the observed patterns. Note that the central TEM_{00} mode is saturated.

conducted.[13] The strong absorption that we observed in CO_2, O_2, and N_2O may be related to the strong absorption at $\lambda = 1.06$ μm of the oxygen molecule.[14] After the resonator is filled with gas at a given pressure, the laser is locked to the TEM_{00} mode, and as either the gas pressure or the laser power is increased new spatial patterns appear. The patterns are the same for all three gases, exhibit sharp thresholds, and show marked hysteresis. An important observation is that the thresholds for the appearance of the various patterns obey a scaling law in laser power, P, and gas pressure, p. We can express this scaling law as

$$X = (P/P_0)^{\beta}\,(p/p_0)^2, \tag{1}$$

where the value of parameter X determines the condition for the transition from one pattern to another for either increasing or decreasing power or pressure. A large number of patterns were observed, but only four occurred at sufficiently low values of X to allow a full set of data to be obtained. For these patterns, a particular transition was typically observed for four to six different laser intensity and pressure settings in the range 0.9–2.0 atm, and a total of seven transitions were studied. All these transitions could be fitted by the same exponent, β, and we find that for O_2, $\beta = 0.42 \pm 0.02$, and for CO_2, $\beta = 0.63 \pm 0.04$. The errors in β are obtained by a χ^2 fit to the data. Note that the normalization of Eq. (1) is arbitrary and does not affect the value of the exponent β. In Fig. 3 we show the value of X, normalized to unity at the appearance of the first nontrivial pattern, for CO_2; the arrows indicate increasing–decreasing power.

The origin of the pattern formation is the introduction of a distributed diverging lens into the optical cavity. As the gas is heated by the absorption of power from the laser beam, a transverse temperature gradient is established in the gas, and this in turn gives rise to a transverse variation in the refractive index. An approximate solution of the steady-state heat equation accurate for $\rho < 1$ is[15,16] ($\rho = r/w_0$, where r is the radial distance and w_0 is the laser beam-waist radius)

$$T(\rho) - T(0) = -\Lambda\rho^2, \quad \Lambda = \frac{0.7\alpha P}{2\pi\kappa}, \tag{2}$$

where α is the absorption coefficient, P is the incident power, $P = I_0 {w_0}^2 \pi/2$, and κ is the thermal conductivity of the gas. This prediction leads to a parabolic variation in the refractive index:

$$n^2(\rho) - n^2(0) = 2n(0)\,\frac{n-1}{T}\,\Lambda\rho^2 \equiv n^2(0)\,(gr)^2, \tag{3}$$

where g is the gradient of the refractive index as defined in Eq. (3), and thus in the paraxial approximation to a hyperbolic ray trajectory.[17] For small angular displacements this variation is equivalent to a defocusing lens of focal length $f = 1/g^2 L$, where L is the length of the resonator. Noting that α and $(n - 1)$ depend linearly on the gas pressure, using the known values for O_2 and the parameters of our resonator, we can write

$$f = -\frac{32\ \text{m}}{(P/500\ \text{W})\,(p/1\ \text{atm})^2}. \tag{4}$$

This value is to be compared with the focal length of the end mirrors, which is $f = 0.5$ m, showing that the effect of the gas can be treated as a perturbation even at the highest pressure and laser power used. Using Eq. (2), we find that for CO_2 the focal length is five times longer. We note, however, that the scaling exponents β are inversely proportional to the thermal conductivity of O_2 and CO_2 and not to the absorption coefficients. At this time we do not have a model that can predict scaling exponent β. For reference, absorption coefficient α, thermal conductivity κ, and thermal nonlinear coefficient n_p defined through $\Delta n = 2n_p P$ are listed in Table 1.

We believe that the patterns represent diffraction of power from the TEM_{00} mode to higher-order transverse modes, not necessarily Hermite–Gaussian, supported by the resonator geometry. Only a small fraction of the power appears in these modes, whereas the laser frequency continues to remain locked onto the TEM_{00}

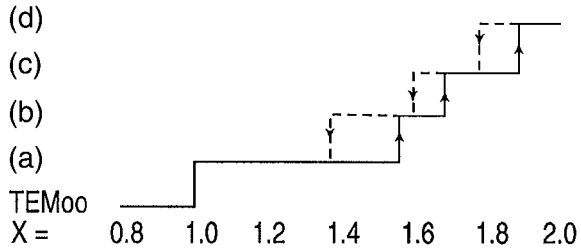

Fig. 3. Parameter X defined in Eq. (1) for the appearance of patterns (a)–(d). Solid curve, increasing power; dashed curve, decreasing power. The typical error in threshold values of X is ~3%.

Table 1. Thermal and Optical Properties of CO_2 and O_2

Property	CO_2	O_2
α (cm^{-1})	5.7×10^{-9}	4.2×10^{-8}
κ (mW/cm K)	0.15	0.26
n_p (W^{-1})	-3.8×10^{-11}	-9.6×10^{-11}
β	0.63	0.42

mode. Because of the small level of coupling, any additional nonlinear effect from the higher-order modes should be negligible. In the far field we observe the same pattern as in the near field and thus are able to perform an accurate estimate of the diffraction angle. From that we find that the equivalent diffraction aperture is $r = 0.2$ mm, equal to the waist of the laser beam in the resonator.

To examine the range of transverse modes that can be supported by the resonator we consider transverse Hermite–Gaussian modes of index (n, m, l). For such modes the resonance frequency is

$$\nu = \frac{c}{2L}\left[n + (1 + m + l)\frac{1}{\pi}\left(\frac{2L}{R}\right)^{1/2}\right], \qquad (5)$$

where L is the length of the resonator and R is the curvature of the (focusing) mirrors. For our resonator $(1/\pi)(2L/R)^{1/2} = 0.142$, so that modes with $(m + l) = 7$ or multiples thereof are close enough in frequency to a TEM_{00} mode to be supported by the resonator. As $(m + l)$ increases, so does the angular divergence of the mode, in agreement with the observation.

The onset of increasingly complex patterns with increasing power and the eventual instability at high power are reminiscent of the approach to chaos in systems governed by nonlinear equations.[18] In a recent publication, Bolda *et al.*[19] analyzed theoretically a system very similar to that of our experiment. They considered a Fabry–Perot resonator with a negative nonlinear refractive index in a cylindrical region on the resonator axis. They found that, when the incident beam was switched off, vortices appeared in the field distribution, giving rise to a distinct pattern in the transverse plane.

We thank T. Blalock for assistance in this experiment and B. Barish, S. Whitcomb, and J. Camp for the loan of the nonplanar ring oscillator laser. This work was supported in part by U.S. Department of Energy grant DE-FG02-91ER40685 and U.S. Air Force Office of Scientific Research contract F49620-00-1-0061. The work was carried out at the Laboratory for Laser Energetics of the University of Rochester. S. J. Bentley's e-mail address is sbentley@optics.rochester.edu.

References

1. C. O. Weiss, M. Vaupel, K. Staliunas, G. Slekys, and V. B. Taranenko, Appl. Phys. B **68,** 151 (1999).
2. J. V. Moloney, H. Adachihara, R. Indik, C. Lizarraga, R. Northcutt, D. W. McLaughlin, and A. C. Newell, J. Opt. Soc. Am. B **7,** 1039 (1990).
3. R. G. Harrison, W. Lu, D. S. Lim, D. Yu, and P. Ripley, Proc. SPIE **2039,** 91 (1993).
4. M. Vaupel, A. Maitre, and C. Fabre, Phys. Rev. Lett. **83,** 5278 (1999).
5. G. Martin and R. W. Hellwarth, Appl. Phys. Lett. **34,** 371 (1979).
6. J. O. Tochio, W. Sibbett, and D. J. Bradley, Opt. Commun. **37,** 67 (1981).
7. H. J. Hoffman, J. Opt. Soc. Am. B **3,** 253 (1986).
8. V. I. Bespalov, A. A. Betin, E. A. Zhukov, O. V. Mitropol'sky, and N. Y. Rusov, IEEE J. Quantum Electron. **25,** 360 (1989).
9. S. J. Bentley, R. W. Boyd, W. E. Butler, and A. C. Melissinos, Opt. Lett. **25,** 1192 (2000).
10. D. Jacob, M. Vallet, F. Bretenaker, A. Le Floch, and R. Le Naour, Appl. Phys. Lett. **66,** 3546 (1995).
11. A. C. Nilsson, E. K. Gustafson, and R. L. Byer, IEEE J. Quantum Electron. **25,** 767 (1989).
12. R. W. P. Drever, J. L. Hall, F. B. Kowalsky, J. Hough, G. M. Ford, A. J. Munley, and H. Ward, Appl. Phys. B **31,** 97 (1983).
13. Absorption data for N_2, O_2, and CO_2 is given in Ref. 9; by the same technique, we found Ar and He to have less absorption than N_2, while absorption for N_2O was of the same order as CO_2.
14. A. R. W. McKellar, N. H. Rich, and H. L. Welsh, Can. J. Phys. **50,** 1 (1972).
15. J. P. Gordon, R. C. C. Leite, R. S. Moore, S. P. S. Porto, and J. R. Whinnery, J. Appl. Phys. **36,** 3 (1965).
16. J. Heebner, Institute of Optics, University of Rochester, Rochester, N.Y. (personal communication).
17. Y. Suematsu and K.-I. Iga, *Introduction to Optical Fiber Communications* (Wiley, New York, 1982).
18. J. Boyce and R. Y. Chiao, Phys. Rev. A **59,** 3953 (1999).
19. E. L. Bolda, R. Y. Chiao, and W. H. Zurek, Phys. Rev. Lett. **86,** 416 (2001).